A.S. Ghatpande · S.K. Sikdar

# Voltage-dependent gating of veratridine-modified RIIA $Na^+$ channel α subunit expressed heterologously in CHO cells

**Abstract** The voltage-dependent kinetics of veratridine-modified RIIA $Na^+$ channel α subunit expressed heterologously in CHO cells were studied using the whole-cell patch-clamp technique. The activation and deactivation kinetics are well described by double exponential functions but poorly by a monoexponential function. Unlike the slow component, the fast time constant and associated amplitude factor depended steeply on the potential. The steady-state activation of veratridine-modified channels is described by a Boltzmann function with a $V_{1/2}$ of –131.9 mV and a slope of 9.41 mV. A two-state model is proposed for the fast component that explains the kinetics of veratridine's mechanism of action.

**Key words** Kinetic analysis · Patch clamp · RIIA sodium channel α subunit · Veratridine-induced modification

## Introduction

Veratridine (VTD) is an alkaloid isolated from the rhizomes of *Veratrum album* or the seeds of *Schoenocaulon officinale*. Along with other "alkaloid" toxins like batrachotoxin, aconitine and various grayanotoxins, VTD is known to bind to the pharmacological site 2 of voltage-sensitive sodium channels [1]. Upon VTD binding, the channels exhibit altered voltage sensitivity, exponential kinetics of activation, loss of selectivity for sodium and loss of fast inactivation (reviewed in [12]).

Studies of the macroscopic voltage-dependent kinetics of VTD-modified sodium currents have been done on frog skeletal muscle [5] and the frog myelinated nerve [6]. The VTD-modified muscle sodium currents exhibit biphasic activation and deactivation, occurring in the millisecond range. In contrast, modified sodium currents in nerve show two types of voltage-dependent gating, one occurring in the millisecond and the other in the seconds' range. The cause of this differential behavior remains unknown. The different kinds of channels and channel-modulating influences present in these excitable preparations may account for this variability in kinetics. Another possibility, suggested by Rando [6], is that channels in different kinetic states interact with VTD, giving rise to different kinetic behavior.

In order to overcome the limitations of excitable preparations, we have investigated the kinetics of the VTD-modified rat brain type IIA sodium channel α subunit expressed heterologously in CHO epithelial cells. Our findings indicate, somewhat surprisingly, the modified RIIA brain sodium channels exhibit kinetics closer to those of modified skeletal muscle sodium currents and that possibly at least two populations of VTD-modified channels coexist, which have very different kinetics and voltage-dependent behavior.

A.S. Ghatpande · S.K. Sikdar (✉)
Molecular Biophysics Unit,
Indian Institute of Science,
Bangalore 560012, Karnataka, India
e-mail: sks@mbu.iisc.ernet.in
Fax: +91-080-3348535

## Materials and methods

### Whole-cell voltage clamp, data acquisition, and analysis

CNa18 cells [7] stably expressing the RIIA sodium channel α subunit were maintained as described previously [2]. Cells were divided into 35 mm dishes, grown to 40–60% confluence and used for whole-cell patch-clamp recordings. Bath solution contained (mM) 137.5 NaCl, 5 HEPES, 1 $MgCl_2$, 1.5 $CaCl_2$. Osmolarity was maintained at 290 mosmol/kg by adjusting the glucose concentration. The pH was adjusted to 7.4 using NaOH. Appropriate amounts of 1 mM VTD stock solution, prepared using the bath solution, were added to the bath to give final concentrations of 100 or 200 µM. The pipette solution contained (mM): 137.5 NaCl, 5 HEPES, 5 EGTA, and 0.5 $CaCl_2$. Osmolarity was maintained at 290 mosmol/kg by adding CsF to the solution. Bath and pipette solutions were filtered through a 0.22 µm filter before use. Micropipettes were pulled from thin-walled, omega dot capillaries (Clarke Electromedical Instruments) and had an average resistance of 1.15–1.25 MΩ. Average cell capacitance was 20 pF, as read from the slow capacitance meter of the EPC 7 patch-clamp amplifier after series resistance compensation of 65–70%. To minimize series resistance effects we recorded from cells only if the uncom-

pensated slow capacitative decay was around 200 µs. Data acquisition was as described previously [2]. Data were filtered at 2 kHz. Curve fitting and data plotting were done in WCP (John Dempster, Strathclyde) and SigmaPlot v 1.02. (Jandel Scientific, Calif., USA). Results are described as mean ±SEM.

VTD-modified channels were generated by a single depolarizing pulse to 0 mV, instead of a train of depolarizing pulses as used in earlier studies [4,5]. All recordings were done from cells equilibrated in 100 or 200 µM VTD to generate a sufficient number of modified channels. High concentrations of VTD along with the single depolarizing pulse to generate VTD-modified channel activity reduce variability in the number of channels modified by VTD. In addition, we normalized the data wherever appropriate to eliminate the remaining small variability. The holding potential ($V_h$) was usually kept at –90 mV unless otherwise mentioned. For the time course analysis, the currents were normalized with respect to the peak current during the pulse and then fitted to a mono or biexponential function (Eqs. 1and 2) of the type:

$$I(t)=a_1\cdot\exp(-t/\tau)+ss \quad (1)$$

or

$$I(t)=a_1\cdot\exp(-t/\tau_1)+a_2\cdot\exp(-t/\tau_2)+ss \quad (2)$$

where ss represents the steady-state current. Similar analysis was done for the activation time course of VTD-modified sodium currents.

Analysis for the steady-state activation was done in the following manner. The tail currents (marked with an asterisk in Fig. 2A) at the end of the hyperpolarizing voltage pulse were fit to a biexponential function (Eq. 3) of the type:

$$I(t)=a_1\cdot\exp(-t/\tau_1)+a_2\cdot\exp(-t/\tau_2)+c \quad (3)$$

The sum $m=a_1+a_2+c$ was taken as a measure of the steady-state fraction of channels open at the end of the hyperpolarizing pulse. The normalized $m$ was plotted against the hyperpolarizing pulse potential and fit with a Boltzmann function (Eq. 4) of the type:

$$f=1/\{1+\exp[(V_{1/2}-V)/k]\} \quad (4)$$

Where $V_{1/2}$ is the potential of half activation and $k$ is a slope factor. Due to a fraction of channels remaining open at –170 mV, the steady-state activation showed a pedestal of 10%. We, therefore, fixed the value of $m$ at –170 mV to zero. The steady-state activation curve for control was generated using the values of $V_{1/2}$ and $k$ as reported previously [8].

The elementary rate constants plotted in Fig. 6 are based on the model of fast activation of VTD-modified channels as described in the Discussion. The values are calculated for VTD-modified channels from Eqs. 5 and 6:

$$\alpha_m=m_\infty/\tau_m \quad (5)$$

and

$$\beta_m=(1/\tau_m)-\alpha_m \quad (6)$$

The plots for the control data were generated using equations reported previously [8].

## Results

Figure 1 shows a sodium current trace at a membrane potential of –20 mV recorded from a CNa18 cell equilibrated in a bath solution containing 200 µM VTD. The transient fast activating sodium current is followed by a characteristic steady inward current. At the end of the depolarizing pulse, a large inward tail current is seen. These two features indicate a loss of fast inactivation and a hyperpolarizing shift of activation due to VTD-induced modification of sodium channels [11]. We have studied the macroscopic kinetics of these VTD-modified channels as described below.

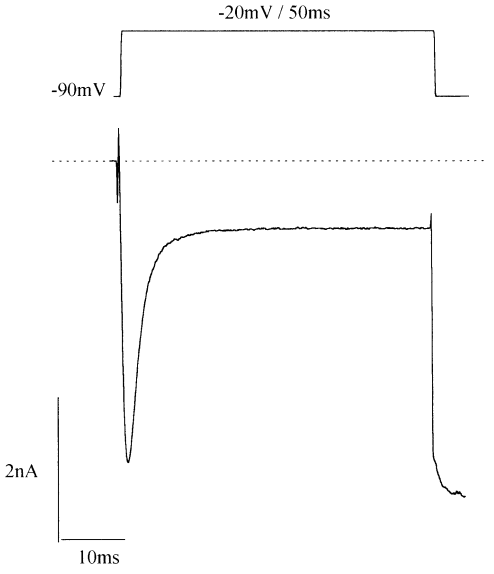


**Fig. 1** Effect of veratridine (*VTD*) on macroscopic RIIA currents. The current trace recorded from a CNa18 cell with 200 µM VTD in bath. Holding potential ($V_h$) was –90 mV and the test pulse was to –20 mV and lasted 50 ms

### Time course of deactivation and activation of VTD-modified sodium currents.

Figure 2A shows an experiment to study the deactivation of VTD-modified RIIA channels. A schematic of the voltage pulse protocol is shown in the upper part of the panel. The current trace shown starts after the prepulse. At the end of the prepulse, a large standing current is seen at the holding potential which is due to VTD-induced modification of sodium channels within the prepulse. These modified channels then deactivate depending on the test pulse potential. A fraction of the channels does not close even at the most hyperpolarizing potential (–170 mV) in 47 ms.

Deactivation is biphasic at all potentials as seen in Fig. 2A. The hollow circles superimposed on some traces indicate a biexponential fit as described in Materials and methods. The time constants and amplitudes from the fit are plotted in Fig. 2B and C. The fast time constant $\tau_1$ shows a steep dependence on potential varying from 0.85±0.06 ms at –169 mV to a $\tau_{max}$ of 3.36±0.46 ms at –130 mV. This corresponds to an e-fold change in 27 mV. The slower time constant $\tau_2$ varies from 21.8±2.1 ms (–135.2 mV) to 31.9±6.6 ms (–164.2 mV) and is 23±9.8 (mean ±SD; $\tau_2/\tau_1$ range: 7.35–32.5) times greater than the fast time constant. Comparatively large errors seen in $\tau_2$ are possibly because of the smaller amplitude associated with the slow component as shown in the next figure. This component shows no definite trend with potential in the range studied.

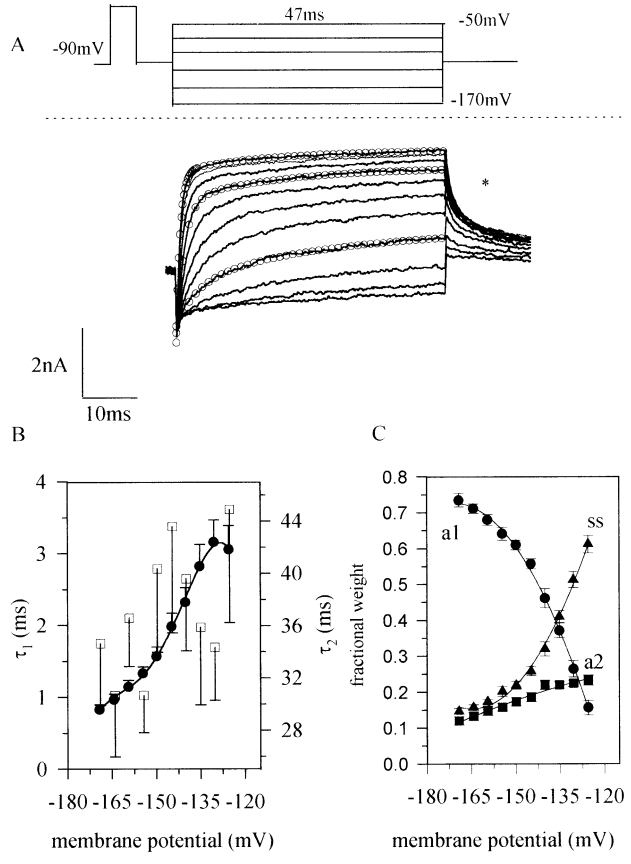


**Fig. 2A–C** Deactivation of VTD-modified channels. **A** *Upper part* of *panel* shows a schematic of the voltage protocol used to record deactivation of VTD-modified channels (*lower part* of *panel*). From a $V_h$ of –90 mV, a depolarizing prepulse to 0 mV was given for 4 ms. After a step to $V_h$ for 10 ms, test pulses of 47 ms duration were applied from a potential of –170 mV to –50 mV in steps of 5 mV. The resulting currents (*dashed line* is baseline) were analyzed for their kinetics by fitting them to biexponential functions (shown as superimposed *open circles* for –170, –155 and –135 mV). Currents up to potential of –125 mV are shown. The currents at the end of the hyperpolarizing pulses (*asterisk*) were analyzed for steady-state activation. **B, C** Plot of fast time constant, $\tau_1$ (*closed circles* in **B**), associated fractional amplitude factor, $a_1$ (*closed circles* in **C**); slow time constant, $\tau_2$ (*open squares* in **B**), associated fractional amplitude factor, $a_2$ (*closed squares* in **C**) and fractional steady-state current amplitude, *ss* (*closed triangles*). *n*=10 cells. *Ordinates* for the two time constants are different

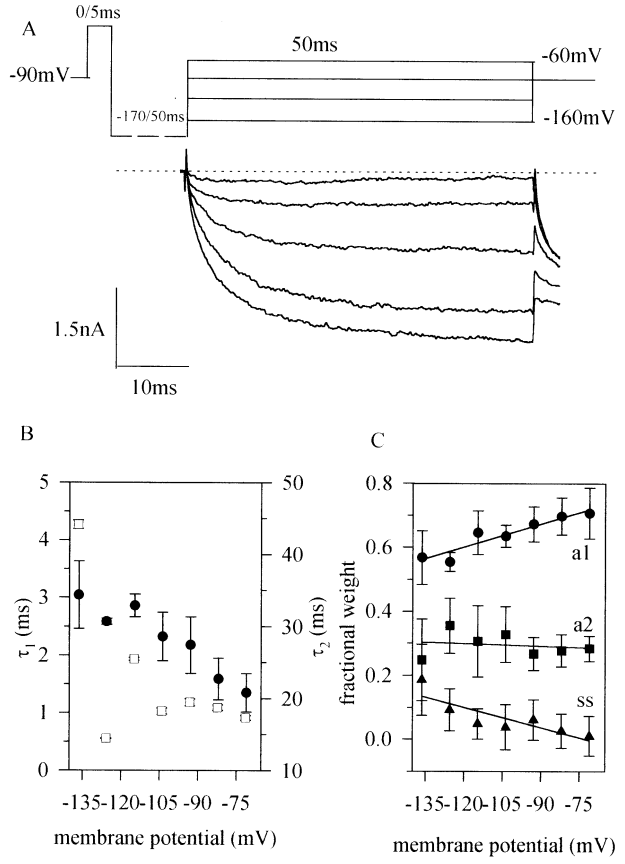


**Fig. 3A–C** Activation of VTD-modified channels. **A** *Upper part* of *panel* is a schematic of the voltage pulse protocol used to record the activation of VTD-modified channels (*lower part* of *panel*). From a $V_h$ of –90 mV, a depolarizing prepulse was given to 0 mV for 5 ms. After a step to –170 mV for 50 ms (shown as a *broken line* in the voltage protocol), test pulses of 50 ms duration were applied from –160 mV to –60 mV in steps of 15 mV. Activating currents, shown for –136.3, –125.4, –114.5, –103.6, –92.7 mV test potentials, were analyzed for their kinetics by fitting them to biexponential functions. **B, C** Plot of the fast time constant of activation, $\tau_1$ (*closed circles* in **B**), associated fractional amplitude factor, $a_1$ (*closed circles* in **C**); slow time constant of activation, $\tau_2$ (*open squares* in **B**), associated fractional amplitude factor, $a_2$ (*closed squares* in **C**), and fractional steady-state current (*closed triangles*) with potential. *n*=3 cells. *Ordinates* for the two time constants are different

The relative amplitudes associated with the two components are shown in Fig. 2C. Amplitude $a_1$, associated with the fast time constant, and the steady-state current ss are mirror images of each other, i.e. a fractional decrease in $a_1$ is reflected as a proportional increase in the steady state. In contrast, the amplitude factor $a_2$, associated with the slower time constant, does not show a strong potential dependence, varying from 10% to 22% in the potential range studied.

Activation of VTD-modified RIIA channels was studied using a voltage protocol shown schematically in the upper part of Fig. 3A. A prepulse was given to open and modify the channels by VTD. This was followed by a midpulse to –170 mV of duration 50 ms, which shuts about 90% of the channels. From this hyperpolarizing potential, the membrane was depolarized to various potentials, which results in the opening of VTD-modified channels. The current traces shown in the lower part of Fig. 3A do not show the prepulse current. The traces shown have been analyzed by setting the current at the end of the –170-mV hyperpolarizing pulse as zero current to correct for the fraction of channels which remain open at –170 mV (see Fig. 2A). Activation of VTD-modified RIIA channels is well described by a biexponential function. Plots of the amplitudes, steady state and time constants from the biexponential fits are shown in Fig. 3B, C. The fast time constant (Fig. 3B) ranges from 3.04±0.58 ms at –136 mV to 1.04±0.33 ms at –71 mV,

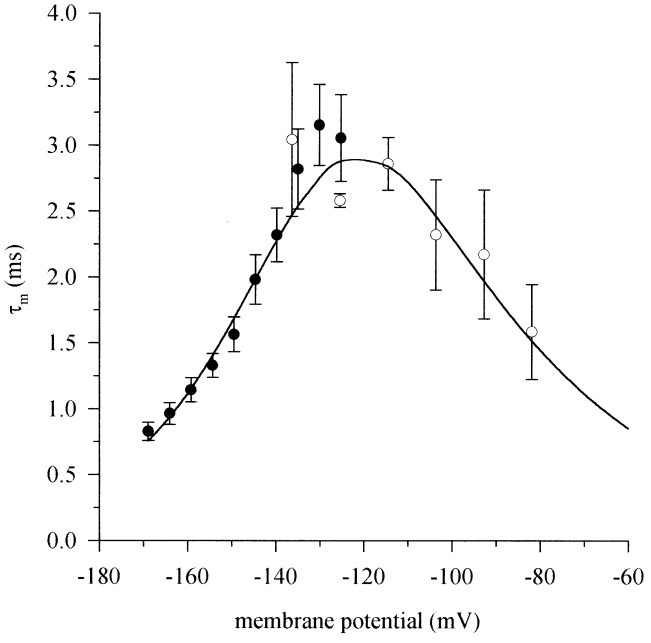


**Fig. 4** Plot of fast time constants as a function of potential. The fast time constants of deactivation (*closed circles*) and activation (*open circles*) plotted as a function of membrane potential. The line passing through the points is a fit by $1/(\alpha_m+\beta_m)$, where $\alpha_m$ and $\beta_m$ are derived from the fits shown in Fig. 6

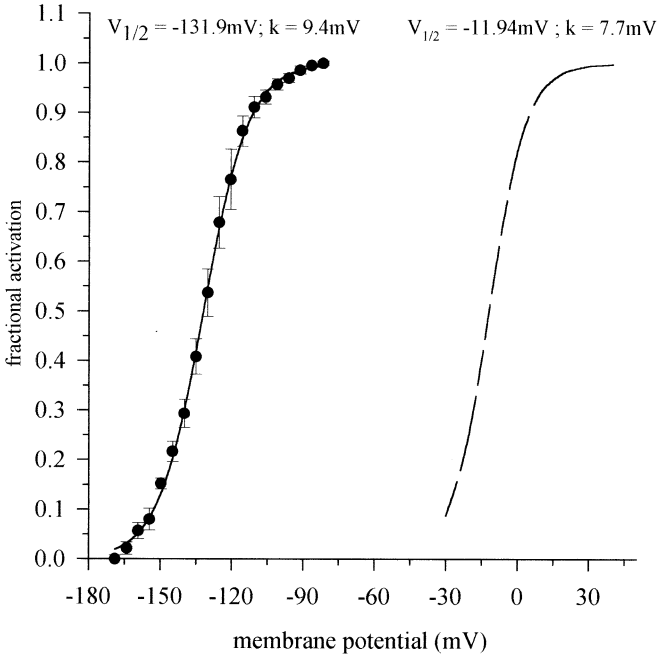


**Fig. 5** Steady-state activation of VTD-modified channels. Fractional steady-state activation of VTD-modified channels (*closed circles*) $n$=6 cells. The line is a fit by the Boltzmann function $f=1/\{1+\exp[(V_{1/2}-V)/k]\}$. The *dashed line* is a theoretical line for fractional steady-state activation of unmodified RIIA sodium channels

corresponding to an e-fold decrease in 83 mV. The slower time constant (Fig. 3C) is seen to be independent of membrane potential with a mean value of 18.92±1.48 ms excluding the value at –135 mV. The slow time constant is 10.05±3.10 (mean ±SD) times the fast time constant. The amplitude factor $a_1$, associated with the fast time constant, increases as a function of membrane potential with a concomitant decrease of steady-state current. The amplitude factor $a_2$, associated with the slower time constant, does not show a definite trend with respect to the membrane potential but has a greater value than in the deactivation experiments.

Figure 4 shows a plot of the fast time constants of deactivation and activation plotted together as a function of membrane potential. These time constants lie on a bell-shaped curve described by $1/\alpha_m+\beta_m$ where $\alpha_m$ and $\beta_m$ are the elementary opening and closing time constants as described in the Discussion.

### Steady-state activation of VTD-modified RIIA sodium channels

Steady-state activation was estimated from the currents at the end of the 47-ms deactivating voltage pulse shown in Fig. 2A. The estimate of fractional activation is described in the Materials and methods. Figure 5 shows a plot of fractional activation of VTD-modified RIIA channels as a function of membrane potential. The data are well described by a Boltzmann function with $V_{1/2}$=–131.9 mV and $k$=9.41 mV. For comparison, the steady-state activation of unmodified RIIA channels is shown [8] which has a $V_{1/2}$ of –12 mV and a slope $k$=7.7 mV. Activation of VTD-modified RIIA sodium channels is shifted by –120 mV in the hyperpolarizing direction and is less steeply potential dependent as compared to the control. The steady-state activation shown has been corrected (Materials and methods) for a pedestal of 10% which arises due to the steady-state current seen even at very hyperpolarized potentials (Fig. 2A).

## Discussion

### Voltage dependence of activation and deactivation of VTD-modified RIIA sodium channels

We studied the rapid, voltage-dependent activation and deactivation gating of the VTD-modified rat brain type IIA sodium channel α subunit expressed heterologously in CHO cells. Our study benefits from the fact that we are fairly sure of the preparation's purity in terms of the type of voltage-activated channels present in the membrane. Earlier work from our laboratory [7] has shown that CHO cells, used to generate the CNa18 cell line, do not carry any message for an endogenous sodium channel homologous to RIIA channels. Isom et al. [4] have shown, using a variety of methods, that CHO cells do not express the $\beta_1$ subunit. It is unlikely that the $\beta_2$ subunit

alone is expressed in these epithelial cells. Taken together, these results indicate that VTD-induced modification of the α subunit alone manifests almost all the effects seen in excitable preparations.

The qualitative features of the kinetics of VTD-modified RIIA and frog skeletal muscle sodium channel are similar although there are quantitative differences. In contrast, the modified nerve sodium channels of frogs [6] show only a single fast component quantitatively comparable to the fast component in skeletal muscle sodium channels and qualitatively comparable to the fast component of modified RIIA channels. Our study demonstrates that biphasic activation and deactivation of VTD-modified channels is intrinsic to the α subunit of voltage-gated sodium channels, i.e. it does not arise because of unknown channels and modulatory influences present in excitable cells. The differences in kinetics reported are probably more attributable to isoform differences in sodium channels from different tissues.

No unique kinetic scheme can be arrived at, based on these data and those obtained previously. Amongst the various possibilities that exist, two are listed below:

1. A linear scheme of two open and closed states connected serially, as proposed by Leibowitz et al. [5].
2. The channels might interact with VTD in two different ways depending on their initial kinetic state. These two distinct populations might give rise to different kinetics and may be mutually exclusive as suggested by Rando [6].

We favor the proposal that there may be two populations of VTD-modified RIIA sodium channels corresponding to each of the two components based on the following considerations.

In the study of myelinated nerve of frog, Rando [6] found two distinct modes of gating, fast and slow, of VTD-modified currents. The slow form of gating interpreted as arising from VTD binding to non-modified, inactivated channels showed a much shallower voltage dependence compared to the rapid form of VTD-modified channels or the unmodified channels. This is analogous to our observation that the slow component is almost independent of membrane potential, although the time-scale of the slow components between the two preparations differs by many orders of magnitude. It is more difficult to imagine a linear kinetic scheme with two closed and open states, because of the large differences in the potential dependence of the two components. This linear scheme would mean that the same gating machinery would have to exhibit large changes in potential-dependent behavior. To observe the gating at the seconds' time-scale in VTD-modified RIIA channels we tried some preliminary experiments using very long depolarizations but were unable to maintain seals.

Open states corresponding to the two populations of channels might also exhibit a distinct conductance. In a single-channel study of guinea pig cardiac myocytes, Sunami et al. [10] found two populations of channels corresponding to distinct conductance levels that exhibit different kinetics and sensitivity to tetrodotoxin. Grayanotoxins (GTX) bind to the same site on sodium channels as other alkaloid toxins [1]. Voltage-clamp studies done on internally perfused squid giant axons by Seyama and Narahashi [9] reveal that GTX I treatment gives rise to two populations of channels. One population gates on the fast time-scale (similar to unmodified channels) but activates at hyperpolarizing potentials. The second population of channels gates in the 100-ms time-scale and has different kinetic properties to the modified channel population, which shows fast gating. Resolution of these issues requires further experimentation.

A fraction of the modified channels does not close in 50 ms, even at the most hyperpolarizing potential (–170 mV). Earlier studies by Leibowitz et al. (Fig. 1 A; [5]) on the frog skeletal muscle, and the myelinated nerve [6] show a similar current at much hyperpolarized potentials. Rando [6] analyzed this current and found that it is present up to –200 mV and is blocked by TTX. He suggested that it may be due to a population of modified channels that does not show voltage-dependent gating, or to an open state stabilized at very negative potentials. We are sure that this current component is not due to artifactual leak subtraction because of its considerable magnitude, which would then have been reflected in a varying baseline. Moreover, this current was present in all the cells analyzed in this fashion (ten cells). Thus, the source of this component still remains unclear but it is not artifactual leak subtraction.

## Mechanism of VTD action

Based on the observation that the two components depend differently on potential and the significant difference in the magnitude of their two time constants, we propose a simple two-state model to explain the voltage dependence of the channel population that shows a strong voltage dependence. The model (Scheme 1) is as follows:

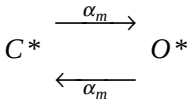


The C* state represents a VTD-modified closed state and the O* is the modified open state with $\alpha_m$ and $\beta_m$ being the forward and backward rate constants respectively.

The rate constants calculated (Materials and methods) from the steady state and the kinetic data are shown in Fig. 6. The elementary rate constants for unmodified channels are also shown for comparison. Fitting the rate constants by the exponential functions described in Materials and methods and extrapolating to the potential range in which the unmodified channels gate, we deduce a plausible mechanism of action for VTD. The opening rate constant, $\alpha_m$, shows a significant value at the normal resting potentials (e.g. –70 mV) of excitable cells, whereas the closing rate constant $\beta_m$ is infinitesimally small at these potentials. This would force the channel

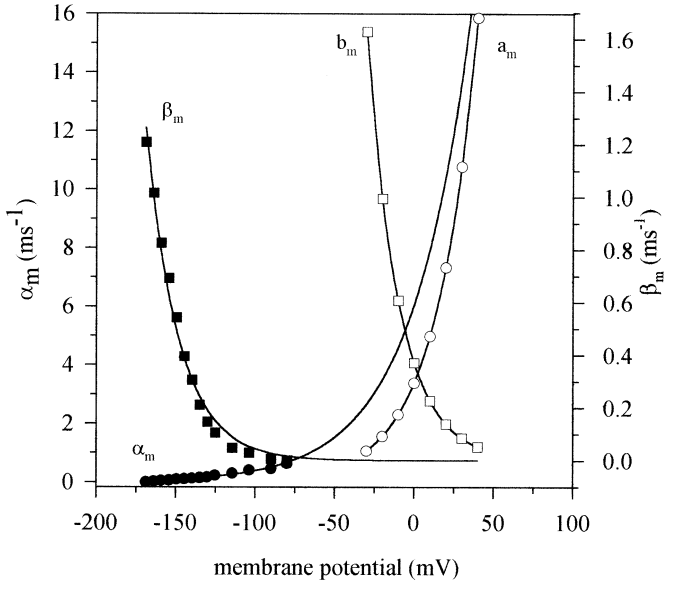


**Fig. 6** Plot of opening and closing rate constants of VTD-modified channels. Elementary rate constants of VTD-modified channels, $\alpha_m$ (*closed circles*), $\beta_m$ (*closed squares*) and unmodified channels $a_m$ (*open circles*), $b_m$ (*open squares*). The *lines* are fits by the equation $s_m = s^o_m \cdot \exp(zFV/RT)$ where $s_m$ is $\alpha$, $\beta$ or *a*, *b*. The fit parameters are, $\alpha_m$: $\alpha^o_m$=3.82 ms$^{-1}$, *z*=0.532; $\beta_m$: $\beta^o_m$=0.00034 ms$^{-1}$, *z*=–1.2; $a_m$: $a^o_m$=3.38 ms$^{-1}$, *z*=0.95; $b_m$: $b^o_m$=0.371 ms$^{-1}$, *z*=–1.22

open at normal resting potentials, leading to sodium influx thereby depolarizing the membrane.

This mechanism of action is similar to that proposed for batrachotoxin [3] and possibly all the alkaloid toxins have a similar kinetic mechanism of action.

In conclusion, VTD-modified channels probably exist as two distinct populations that have different kinetics and potential dependence and may have different conductances and TTX sensitivity as well. VTD exerts its action by selectively affecting the closing rate of sodium channels such that the channels remain open at normal resting membrane potentials.

**Acknowledgements** ASG is a Senior Research Fellow of C.S.I.R. India. This research was supported by grants from C.S.I.R. and Department of Science and Technology, India. The equipment was partly financed by the Erna and Victor Hasselblad Foundation, Sweden.

## References

1. Catterall WA (1977) Activation of the action potential $Na^+$ ionophore by neurotoxins. An allosteric model. J Biol Chem 252:8669–8676
2. Ghatpande AS, Sikdar SK (1997) Competition for binding between veratridine and KIFMK: an open channel blocking peptide of the RIIA sodium channel. J Membr Biol 160:177–182
3. Khodorov BI (1985) Batrachotoxin as a tool to study voltage-sensitive sodium channels of excitable membranes. Prog Biophys Mol Biol 45:57–148
4. Isom LL, Scheuer T, Brownstein AB, Ragsdale DS, Murphy BJ, Catterall WA (1995) Functional co-expression of the beta 1 and type IIA alpha subunits of sodium channels in a mammalian cell line. J Biol Chem 270:3306–3312
5. Leibowitz MD, Sutro JB, Hille B (1986) Voltage-dependent gating of veratridine-modified channels. J Gen Physiol 87: 25–46
6. Rando TA (1989) Rapid and slow gating of veratridine-modified sodium channels in frog myelinated nerve. J Gen Physiol 93:43–65
7. Sarkar SN, Sikdar SK (1994) High level stable expression of rat brain type IIA sodium channel $\alpha$ subunit in CHO cells. Curr Sci 67:196–199
8. Sarkar SN, Adhikari A, Sikdar SK (1995) Kinetic characterization of rat brain type IIA sodium channel $\alpha$ subunit stably expressed in CHO cells. J Physiol (Lond) 488:633–645
9. Seyama A, Narahashi T (1981) Modulation of sodium channels of squid nerve membrane by grayanotoxin I. J Pharmacol Exp Ther 219:614–624
10. Sunami A, Sasano T, Matsunaga A, Fan Z, Sawanobori T, Hiraoka M (1993) Properties of veratridine-modified single $Na^+$ channels in guinea pig ventricular myocytes. Am J Physiol 264:H454–H463
11. Sutro JB (1986) Kinetics of veratridine action on Na channels of skeletal muscle. J Gen Physiol 87:1–24
12. Ulbricht W (1998) Effects of veratridine on sodium currents and fluxes. Rev Physiol Biochem Pharmacol 133:1–54